# Methyl Cation Affinities

**Terrance B. McMahon,[‡] Thomas Heinis,[†] Gordon Nicol,[†] Jamey K. Hovey,[‡] and Paul Kebarle*,[†]**

*Contribution from the Chemistry Departments, University of Alberta, Edmonton, Alberta, Canada T6G 2G2, and University of Waterloo, Waterloo, Ontario, Canada N2L 3G1.*
*Received March 4, 1988*

**Abstract:** Measurement of the $CH_3^+$ ($Me^+$) transfer equilibria, $B'Me^+ + B = B' + MeB^+$, with a pulsed high-pressure mass spectrometer and an ion cyclotron resonance mass spectrometer led to a scale of relative methyl cation affinities of bases B, MCA(B). This scale when calibrated to the literature value for the $Me^+$ affinity of $N_2$ led to absolute MCA values for the other 24 bases B that were part of the scale. Rate constants for several $Me^+$ transfer reactions were determined also. These were equal to collision rates for large exothermicity of the reactions and decreased below collision rates at low exothermicities. The MCA(B) values follow in general the proton affinities PA(B). A plot of PA(B) vs. MCA(B) leads to a slope of ~3 at low MCA(B) which becomes close to ~1 at high MCA(B). It is shown that this behavior can be rationalized.

This paper presents thermochemical data for the methyl cation ($Me^+$) affinities of bases B, MCA(B), which correspond to the enthalpy change $\Delta H^\circ_1$ for the dilute gas-phase reaction 1. The

$$BMe^+ = B + Me^+ \qquad (1)$$

$$B'Me^+ + B = (B'\cdots\overset{H}{\overset{|}{C}}\cdots B)^+ = B' + MeB^+ \qquad (2)$$
$$\qquad\qquad\qquad\qquad\quad H \quad H$$

$\Delta H^\circ_1$ were obtained through determinations of the $Me^+$ transfer equilibria 2 which are cationic $S_N2$ reactions. The resulting, free energy changes, $\Delta G^\circ_2 = -RT \ln K_2$, could be converted to $\Delta H^\circ_2$ by estimates of the small $\Delta S^\circ_2$ changes. A scale of interconnected $\Delta G^\circ_2$ and also a scale of $\Delta H^\circ_2$ changes were obtained. The $\Delta H^\circ_2$ scale could be converted to a $\Delta H^\circ_1$ scale with use of available literature values of $\Delta H^\circ_1$ for one of the bases B. In this manner MCA(B) for some 25 bases B could be obtained.

The above methodology is analogous to that used for the determination of proton affinities via measurements of proton transfer equilibria.[1a] Proton transfer equilibria measurements have led to proton affinities of literally thousands of compounds.[1,2] On the other hand, previous MCA determinations have been very limited, yet methylation reactions like (2) are of importance in an extremely wide range of research areas. To indicate the scope, one may mention (a) $Me^+\cdot B$ formation by the reverse of (1) in interstellar clouds where B may be Ne, $H_2$, $O_2$, CO, $CO_2$, etc., and the transfer of $Me^+$ to other B via bimolecular reactions (2) and its presumed significance to interstellar molecular synthesis;[3] (b) methylation and alkylation in organic synthesis undertaken in solution with use of diazonium ions,[4] $MeN_2^+$ and $RN_2^+$, or halonium ions,[5] $MeXR^+$; (c) carcinogenicity of alkylating agents, believed to achieve activity by conversion to highly reactive diazonium cations which alkylate nucleophilic sites in DNA.[6]

Although the present studies are for the gas-phase species, they can be of significance also for the understanding of the processes occurring in solution. The gas-phase thermochemical data relate directly to energy changes obtained by quantum chemical computation which provide essential complementary information on structures and energy.[6-8] Furthermore, comparison between the energy changes in the gas phase and solution can be expected to provide important insights into the solvent effects. Certainly this approach has proven most fruitful in the study of gas-phase and solution Brønsted acidities and basicities.[1]

The experimental gas-phase studies of MCA's were initiated by Beauchamp.[9] Significant development using both ICR and high-pressure mass spectrometric techniques has occurred since then and will be considered in the Discussion.

## Experimental Section

Most of the measurements were made with a pulsed electron high-pressure mass spectrometer, PHPMS, which has been described.[10] The experimental conditions and procedures were similar to those used in earlier work.[1a] All measurements were performed at 400 K ion source temperature. At this elevated temperature the formation of ion clusters like $Me^+B_2$ etc. is much reduced and does not interfere with the equilibria measurements.

The gas mixture entering the ion source was passed through a cold trap located close to the ion source. This removed traces of water vapor. The temperature of the trap was varied from −77 to −160 °C depending on the volatility of the bases B used; i.e., the temperature was chosen to be high enough so as to pass through B but retain $H_2O$.

Some of the measurements were performed with an ion cyclotron resonance (ICR) spectrometer which has previously been described in detail.[11,12]

## Results and Discussion

**a. Typical Equilibria Measurements of $Me^+$ Transfer Reactions.** Many of the $Me^+$ transfer equilibria were achieved by producing first the dimethylfluoronium ion, $CH_3FCH_3^+$, and using this ion as the primary reagent in the $Me^+$ transfer. The ion intensities observed in a PHPMS run used to elucidate the reaction sequence leading to $CH_3FCH_3^+$ are given in Figure 1. The major gas is nitrogen and electron impact ionization of $N_2$ leads to $N_2^+$ and $N^+$. In the absence of $CH_3F$, the $N_2^+$ is converted to $N_4^+$ and the $N^+$ to $N_3^+$, within ~50 μs, such that a distribution of $N_4^+$ to $N_3^+$ of 80:20 results.[13] In the present case (see Figure 1), because of the low $CH_3F$ pressure the same conversion occurs almost to completion. Therefore, the ions reacting with $CH_3F$ are predominantly $N_4^+$ and $N_3^+$ in an 80:20 ratio. Probably, the

[†] University of Alberta.
[‡] University of Waterloo.

(1) (a) McMahon, T. B.; Kebarle, P. *J. Am. Chem. Soc.* **1985**, *107*, 2612. (b) Taft, R. W. *Prog. Phys. Org. Chem.* **1983**, *14*, 248. (c) Brauman, J. I. *Annu. Rev. Phys. Chem.* **1983**, *34*, 187, and references therein.
(2) Lias, S. G.; Liebman, J. F.; Levin, R. *J. Phys. Chem. Ref. Data* **1984**, *13*, 695.
(3) (a) Adams, N. G.; Smith, D. *Chem. Phys. Lett.* **1981**, *79*, 563. (b) Smith, D.; Adams, N. G. *Astrophys. J.* **1978**, *L87*, 220.
(4) Keating, J. T.; Skell, P. S. In *Carbonium Ions*; Olah, G., Schleyer, P. v. R., Eds.; Wiley-Interscience: New York, 1970; Vol. II, Zollinger, H. *Azo and Diazo Chemistry*; Interscience: New York, 1961. Zollinger, H. *Acc. Chem. Res.* **1973**, *6*, 335. Krimze, w. *Angew. Chem., Int. Ed. Engl.* **1976**, *15*, 251.
(5) Olah, G. A. *Halonium Ions*; Wiley: New York, 1975.
(6) Ford, G. P.; Scribner, J. D. *J. Am. Chem. Soc.* **1983**, *105*, 349.
(7) Ragharachari, K.; Chandrasekhar, J.; Burnier, R. C. *J. Am. Chem. Soc.* **1984**, *106*, 3124.
(8) Vincent, M. A.; Radom, L. *J. Am. Chem. Soc.* **1978**, *100*, 3306.
(9) Holtz, D.; Beauchamp, J. L.; Woodgate, S. D. *J. Am. Chem. Soc.* **1970**, *92*, 7484.
(10) Kebarle, P. In *Techniques for the Study of Ion-Molecule Reactions (Techniques of Chemistry Series)*; Saunders, W., Farrar, J. M., Eds.; Wiley-Interscience: New York, 1988.
(11) Hovey, J. K.; McMahon, T. B. *J. Am. Chem. Soc.* **1986**, *108*, 1719.
(12) Hovey, J. K.; McMahon, T. B. *J. Phys. Chem.* **1987**, *91*, 4560.
(13) Good, A.; Durden, D. A.; Kebarle, P. *J. Chem. Phys.* **1970**, *52*, 212.

0002-7863/88/1510-7591$01.50/0 

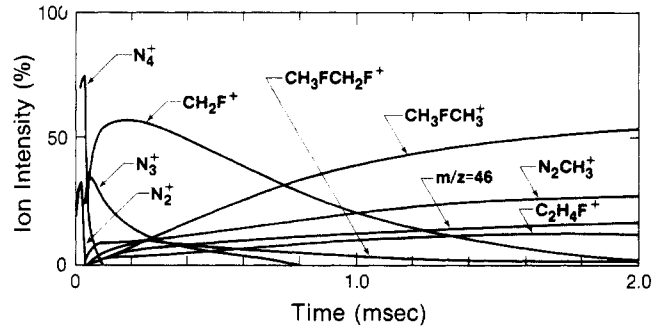


**Figure 1.** Relative ion intensity time dependence after electron pulse. Gases in ion source: $N_2$, 3.5 Torr; $CH_3F$, 0.4 mTorr; $T$ = 400 K. Reaction sequence eq 3–6 (see text) leads to major products $CH_3FCH_3^+$ and $CH_3N_2^+$.

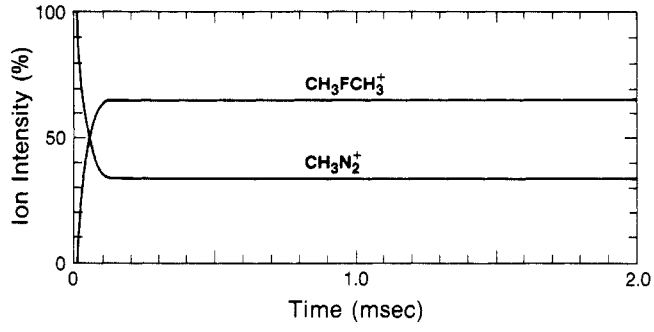


**Figure 2.** At a $CH_3F$ pressure which is 10 times higher than that used in Figure 1, $CH_3FCH_3^+$ and $CH_3N_2^+$ reach equilibrium rapidly: $N_2$, 5 Torr; $CH_3F$, 5 mTorr.

dominant $N_4^+$ produces mostly $CH_2F^+$ ions by the dissociative charge transfer reaction (3); see Figure 1. The fluoromethyl cation

$$N_4^+ + CH_3F \rightarrow 2N_2 + CH_2F^+ + F \quad (3)$$

$$N_4^+ + CH_3F \rightarrow 2N_2 + CH_3F^+ \quad (3a)$$

$$CH_3F + CH_2F^+ + M \rightarrow CH_3FCH_2F^+ + M \quad (4)$$

$$CH_3F + CH_3FCH_2F^+ \rightarrow CH_3FCH_3^+ + CH_2F_2 \quad (4a)$$

$$CH_3FCH_3^+ + N_2 \rightleftarrows CH_3F + CH_3N_2^+ \quad (5)$$

$$CH_3F^+ + CH_3F = CH_3FH^+ + CH_2F \quad (6)$$

$$CH_3FH^+ + CH_3F = CH_3FCH_3^+ + HF \quad (6a)$$

is known[14] not to undergo bimolecular reactions with $CH_3F$. In the present case, the slow disappearance of this cation should be due to the third body dependent association with $CH_3F$ shown in (4). This reaction is followed by the nucleophilic displacement reaction (4a) which leads to the desired dimethylfluoronium ion. In the presence of the large excess of $N_2$, some endothermic $Me^+$ transfer occurs via (5), a reaction that is reversible but which has not yet reached equilibrium in Figure 1. When larger pressures of $CH_3F$ are provided, the ions engaged in the reversible reaction (5) become dominant quite early and reach equilibrium much faster. This is illustrated in Figure 2. Runs under such concentration conditions were used to determine the equilibrium constant $K_5$.

Some $CH_3F^+$ is also produced by charge transfer from $N_4^+$; see reaction 3a. This ion could be observed when the $CH_3F$ pressures were lower than that used in the run of Figure 1. The $CH_3F^+$ disappeared rapidly, presumably by the sequence of bimolecular reactions 6 and 6a which also lead to $CH_3FCH_3^+$. These reactions proceed at near Langevin collision rates; see Beauchamp[15] and Harrison.[16]

(14) Blint, R. J.; McMahon, T. B.; Beauchamp, J. L. *J. Am. Chem. Soc.* **1974**, *96*, 1269.

(15) Beauchamp, J. L.; Holtz, D.; Woodgate, S. D.; Patt, S. L. *J. Am. Chem. Soc.* **1972**, *94*, 2798.

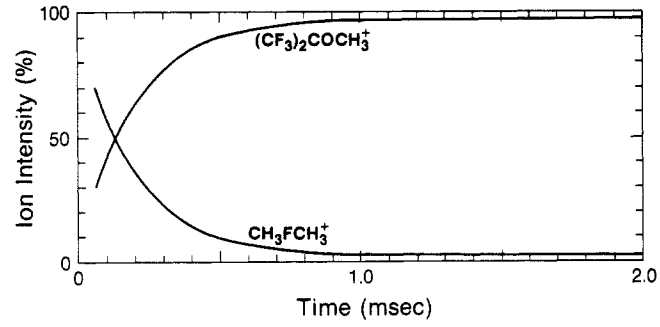


**Figure 3.** Ion intensities observed with $N_2$ (3.5 Torr), $CH_3F$ (33 mTorr), and $(CF_3)_2CO$ (11 mTorr); $T$ = 400 K. The equilibrium $CH_3FCH_3^+ + OC(CF_3)_2 = CH_3F + CH_3OC(CF_3)_2^+$ is reached rather slowly even though $p(CF_3)_2CO$ is relatively high. This is due to a low rate constant of the reaction.

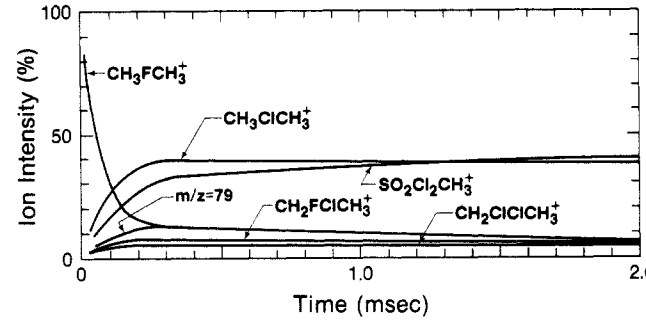


**Figure 4.** Example of a run where $CH_3FCH_3^+$, produced rapidly by reactions 3–6 (see Figure 1 and text), is used to transfer $Me^+$ to two bases, $CH_3Cl$ and $SO_2Cl_2$, which then engage in $Me^+$ transfer equilibrium: $N_2$, 3.5 mTorr; $CH_3F$, 100 mTorr; $CH_3Cl$, 1 mTorr; $SO_2Cl_2$, 1.7 mTorr; 400 K.

**Table I.** Reproducibility of Equilibrium Constant $K_2$ for Different Concentrations of B′ and B[a]

| $p(CH_3Cl)$[b] | $p(SO_2Cl_2)$[b] | $K_2$ |
|---|---|---|
| 5.3 | 1.7 | 1.1 |
| 4.4 | 1.4 | 0.8 |
| 1.2 | 4.0 | 1.1 |
| 0.8 | 2.7 | 1.6 |
| 1.2 | 9.9 | 1.6 |
| 1.2 | 12.6 | 0.8 |
| 1.0 | 10.7 | 1.2 |

[a] For reaction: $CH_3ClCH_3^+ + SO_2Cl_2 = CH_3Cl + SO_2Cl_2CH_3^+$, at 400 K. [b] Ion source pressures in mTorr.

The ion intensities shown in Figure 3 illustrate the measurement of an equilibrium between $CH_3FCH_3^+$ and a base B = perfluoroacetone, which has an MCA that is higher than that of $CH_3F$. The use of relatively high partial pressures for $CH_3F$ leads to rapid production of the dimethylfluoronium ion. The equilibrium 7 is reached after ~1 ms (see Figure 3) even though the

$$CH_3FCH_3^+ + OC(CF_3)_3 = CH_3F + CH_3OC(CF_3)_2^+ \quad (7)$$

perfluoroacetone pressure is relatively high. This result indicates that the rate constant $k_7$ for the forward direction is considerably below the collision limit ($k_7 \approx 2 \times 10^{-11}$ molecule$^{-1}$ cm$^3$ s$^{-1}$). It is shown in the kinetic section that this slow reaction is not an isolated case; i.e., a good fraction of the exothermic $Me^+$ transfer reactions proceed at rates which are considerably below collision rates. Slow $Me^+$ transfer rates make the equilibria measurements more difficult since other faster competitive reactions may change the concentrations of the ions engaged in the $Me^+$ transfer equilibrium.

In the above example $CH_3F$ is one of the bases B engaged in the $Me^+$ transfer equilibrium. Many $Me^+$ equilibria were measured where $CH_3F$ was not one of the bases engaged in the

(16) Herod, A. A.; Harrison, A. G.; McAskill, N. A. *Can. J. Chem.* **1971**, *49*, 2217.

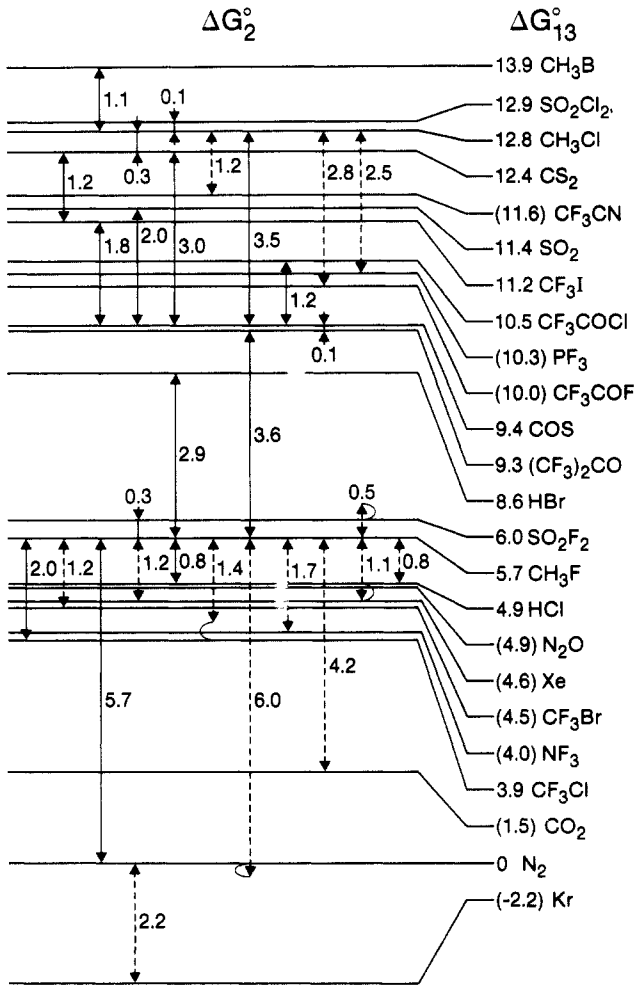


**Figure 5.** Free energy changes $\Delta G°_2$ from equilibrium constants $K_2$ for reactions 2: $B'CH_3^+ + B = B' + CH_3B^+$: solid arrows, PHPMS data at 400 K; dashed arrows, ICR results at 300 K. $\Delta G°_{13}$ values obtained from summation of $\Delta G°_2$ correspond to free energy change for reaction 13: $N_2CH_3^+ + B = N_2 + CH_3B^+$.

equilibrium. Even in these experiments, very often $CH_3FCH_3^+$ was used as the primary methylating agent of the two bases of interest. This was done when both bases had MCA's which were considerably higher than that of $CH_3F$. Typically, the gas mixtures contained $N_2$ as major gas and relatively high pressures (50–100 mTorr) of $CH_3F$, while the two bases B were in the 1–5 mTorr range. Under these conditions reactions 1–6 produced rapidly $CH_3FCH_3^+$ which then transferred $Me^+$ to the two bases. An example of such a run is given in Figure 4 where the two $MeB^+$ at equilibrium are $CH_3ClCH_3^+$ and $CH_3SO_2Cl_2^+$.

In general the concentration of the bases was changed in separate runs and the resulting ion equilibria were measured. Table I illustrates the type of consistency obtained for equilibrium 8,

$$CH_3ClCH_3^+ + SO_2Cl_2 = CH_3Cl + CH_3SO_2Cl_2^+ \quad (8)$$

for which one run was displayed in Figure 4.

In general, the measurement of the $Me^+$ transfer equilibria was considerably more difficult than previous PHPMS proton transfer equilibria measurements. In the proton transfer measurements, conditions could be achieved where the two protonated species represented better than the 80% of the total ion concentration. Furthermore these equilibria almost always proceeded at collision rates in the exothermic direction. In the MCA equilibria, in addition of the two $MeB^+$ ions, often there were other ions produced by obscure reactions. Also, some of the $Me^+$ transfer reactions were slow. For these reasons we have assigned somewhat larger uncertainties to the MCA results. In the most unfavorable cases, relative errors in the $\Delta G°_2$ measurements of ±1 kcal/mol cannot be excluded.

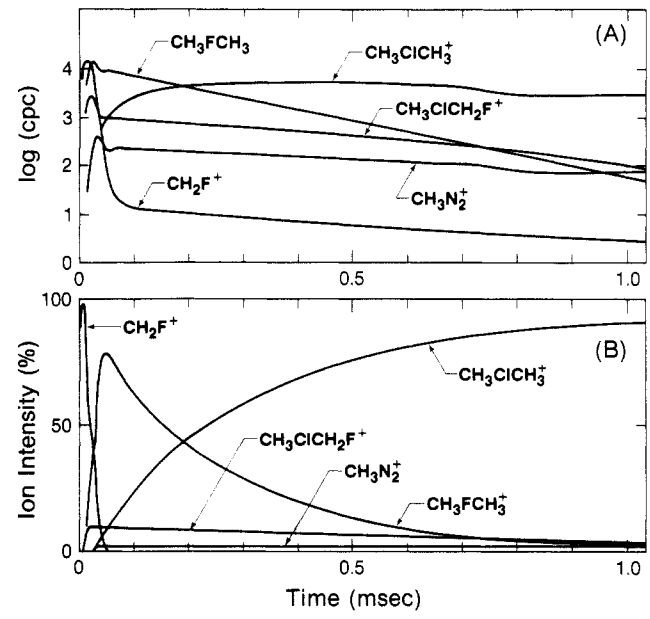


**Figure 6.** Ion intensity time dependence in a run used to determine rate constant $k$ for the reaction $CH_3FCH_3^+ + ClCH_3 = CH_3F + CH_3ClCH_3^+$. (A) The logarithms of the measured ion intensities in counts per channel. The linear decrease of the $CH_3FCH_3^+$ ion is due to the pseudo-first-order $Me^+$ transfer reaction. (B) The corresponding relative intensities in a linear plot.

Equilibrium constants $K_2$ for the general $Me^+$ transfer reaction (2) determined by the measurements described above were used to obtain the corresponding $\Delta G°_2$ values. The resulting ladder of interconnected $\Delta G°_2$ values is shown in Figure 5. The PHPMS results are for 400 K while the ICR are for 300 K. Even though the temperatures are different, the $\Delta G°_2$ can be compared directly since $\Delta S°_2$ is generally small, which means that the temperature effect on the $\Delta G°_2$ is small. In general, there is good agreement between the PHPMS and ICR results; see data for $CF_3Cl$ (within 0.6 kcal/mol), HCl (within 0.4 kcal/mol), and $SO_2F_2$ (within 0.2 kcal/mol), and difference between $N_2$ and $CH_3F$ (within 0.3 kcal/mol) (see Figure 5).

The thermochemical data based on the results in Figure 5 are discussed in sections c and d of the Results and Discussion.

**b. Rate Constants for $Me^+$ Transfer Reactions from $Me_2F^+$ and $Me_2Cl^+$ to Bases B.** The rate constants for several $Me^+$ transfer reactions from $CH_3FCH_3^+$ to different bases B were determined in a number of special experiments where the partial pressure of $CH_3F$ was relatively high, such that formation of $CH_3FCH_3^+$ by reactions 3–6 was rapid, while the pressure of B was relatively low so that the kinetics of the $CH_3B^+$ production by $CH_3^+$ transfer from $CH_3FCH_3^+$ occurred within the time window of the PHPMS. The results from such a typical run are shown in Figure 6, which gives both a logarithmic plot of the absolute intensities and a linear plot of the relative ion concentrations. The logarithmic plot gives a good picture of low intensity ions that are also present, while the linear "normalized" plot provides a picture of the main events, i.e., reaction 9. A plot of

$$CH_3FCH_3^+ + ClCH_3 \rightarrow CH_3F + CH_3ClCH_3^+ \quad (9)$$

the natural logarithm of the normalized intensity of $CH_3FCH_3^+$ vs. time gave a straight line whose slope is identified with $\nu_9$, the pseudo-first-order rate constant. The known concentration of B = $CH_3Cl$ was then used to obtain $k_9$, see eq 10.

$$\nu = k[B] \quad (10)$$

Determinations of $\nu$ at different [B] gave invariant rate constants $k$ for this and the other reactions studied. The results of the kinetic determinations are summarized in Table II. Included in the table are also results from previous determinations[17] of the

(17) Sen Sharma, D. K.; Kebarle, P. *J. Am. Chem. Soc.* **1982**, *104*, 19.

**Table II.** Rate Constants $k$ for Reactions: $Me_2X^+ + B = MeX + MeB^+$

| X | B | $(k \times 10^9)^c$ | $(-\Delta G°)^d$ |
|---|---|---|---|
| $F^a$ | $CH_3Cl$ | 1.4 | 7.1 |
| | $CS_2$ | 1.4 | 6.4 |
| | $SO_2Cl_2$ | 1.0 | 7.2 |
| | $SO_2$ | 0.3 | 5.7 |
| | $SO_2ClF$ | 0.3 | ~5.7[e] |
| | $(CF_3)_2CO$ | 0.02 | 3.6 |
| $Cl^b$ | $(CH_3)_3N$ | 1.2 | 64 |
| | $H_3N$ | 0.8 | 43 |
| | $(CH_3)_2O$ | 1.1 (0.5)[f] | 31 |
| | $C_2H_5OH$ | 0.5 | 27 |
| | $CH_3C_6H_5$ | 0.05 | 34 |
| | $C_6H_6$ | 0.002 | 33 |

[a] Temperature 400 K, present work. [b] Temperature 315 K, from Sen Sharma.[17] [c] In molecule$^{-1}$ cm$^3$ s$^{-1}$. [d] Free energy change of reaction in kcal/mol ($\Delta G° \approx \Delta H°$): for F from Figure 5 and Table III; for Cl from Sen Sharma.[17] [e] Estimate based on assumption that $\Delta G°$ for $SO_2ClF$ should be between $SO_2Cl_2$ and $SO_2F_2$ but closer to $SO_2Cl_2$; see Figure 5. [f] Value for 400 K from Sen Sharma.[17]

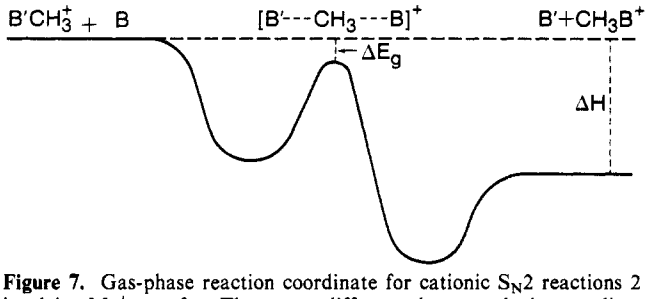


**Figure 7.** Gas-phase reaction coordinate for cationic $S_N2$ reactions 2 involving $Me^+$ transfer. The energy difference between the intermediate $B'CH_3B^+$ and the reactants $B'CH_3^+$ and B, called $\Delta E_g$, controls the rate. A large $-\Delta E_g$ leads to collision rates; a small $-\Delta E_g$ leads to negative temperature dependence and low rates.

rate constants involving $Me^+$ transfer from dimethylchloronium ion to bases B; see eq 11. Examining first the $Me_2F^+$ data in

$$CH_3ClCH_3^+ + B = CH_3Cl + CH_3B^+ \qquad (11)$$

the table, we notice that the rate constants are close to the Langevin–ADO collision limit at higher exoergicities of the reaction and gradually decrease to considerably below the collision limit. Thus for B = perfluoroacetone at an exoergicity of 3.6 kcal/mol, the collision limit is higher by a factor of ~100 than the observed rate. A similar trend is observed for the $Me_2Cl^+$ data; however, in this case, the decrease occurs already at much higher exoergicities. It is most likely that the $Me^+$ transfer reactions 11 and 12 proceed by an $S_N2$ mechanism involving

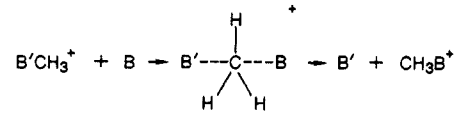


(12)

"backside attack" and inversion of the methyl group.

A double minimum potential well is expected[17-19] for the reaction coordinate in the gas phase as shown in Figure 7. Theoretical calculations also have provided such double minima reaction coordinates; see Chandrasekhar[7] for $Me^+$ transfer from $MeOH_2^+$ to $OH_2$ and to $CH_3OH$. When the gap ($-\Delta E_g$) is large (see Figure 7), the reactions proceed at collision rates. For reactions where the gap is small, the rate is slow and decreases as the temperature is increased (negative temperature dependence);[17] see, for example, data for $Me_2Cl^+$ and B = $Me_2O$ in Table II.

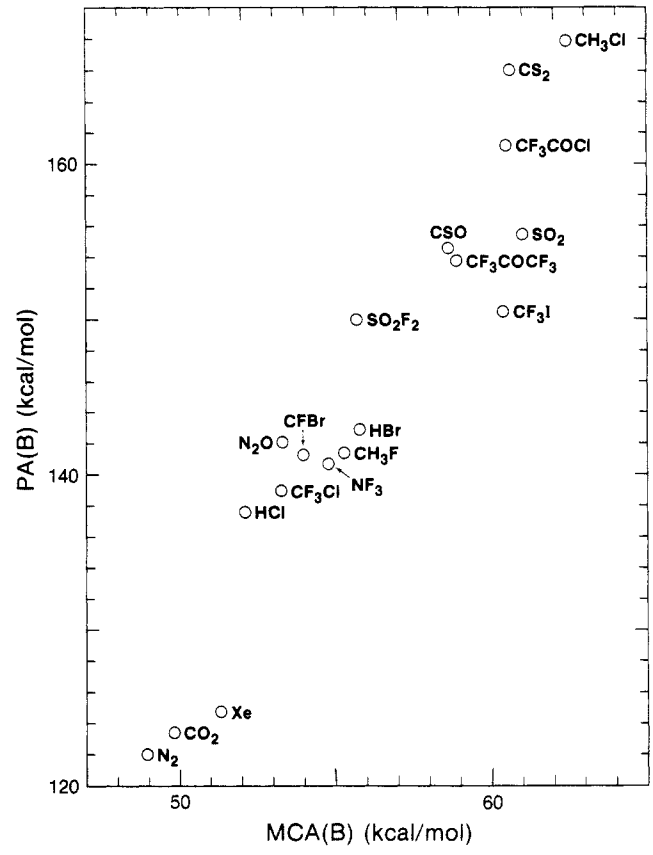


**Figure 8.** Plot of proton affinities PA(B) versus methyl cation affinities MCA(B) for bases of Table III; slope ≈ 3.

For the series of bases below B = $Me_2O$, the gap gradually gets smaller, and for benzene, the gap disappears; i.e., $\Delta E_g$ has become positive and the rate is very low and is found to increase with temperature.[17]

Neglecting entropic factors, a direct relationship between rate and gap width can be expected. The gap width is expected to increase monotonically with increase of reaction exoergicity and thus with the MCA(B) only when a series of related bases B is involved.[20] For example, the bases EtOH to $Me_3N$ (see $Me_2Cl^+$ results in Table II) represent such a group (oxygen and nitrogen bases). The bases toluene and benzene fall in another group (carbon bases) which is much less nucleophilic. Substantial reaction exothermicity still occurs for the latter group owing to resonance stabilization (charge delocalization) present in the products but not in the transition state.[17] This means that the rates for this group are expected to be lower at equal exothermicity, relative to the first group.

The observed decrease of rates for $Me^+$ transfer from $Me_2F^+$ to B with decreasing exoergicity of the reactions, i.e., decreasing MCA(B) (Table II), is thus expected. Even though the nucleophilic centers on the bases involved are fairly dissimilar, still these are systems in which selective resonance stabilization of the products only does not occur to any extent. The experimental observation that for $Me_2F^+$ the rates remain close to collision rates down to very low exothermicities, while for $Me_2Cl^2$ they begin to decrease already at 30 kcal/mol exothermicities (B = $Me_2O$), cannot be attributed to different nucleophilicities of the bases used in the two groups. Thus $Me_2O$ is more nucleophilic than all of the bases of the $Me_2F^+$ group. Obviously the difference must be due to differences between $Me_2F^+$ and $Me_2Cl^+$; i.e., reactions of $Me_2F^+$ would lead to a much larger gap ($-\Delta E_g$) relative to reactions with $Me_2Cl^+$ when the same base B is involved. The observed greater reactivity of $Me_2F^+$ relative to $Me_2Cl^+$ is in line with the lower MCA of MeF relative to the MCA of MeCl; see

(18) (a) Farneth, W. E.; Brauman, J. I. *J. Am. Chem. Soc.* **1976**, *98*, 7891. (b) Olmstead, W. N.; Brauman, J. I. *Ibid.* **1977**, *99*, 4219. (c) Asubiojo, O. I.; Brauman, J. I. *Ibid.* **1979**, *101*, 3715. Pellerite, M. J.; Brauman, J. I. *Ibid.* **1980**, *102*, 5993.

(19) Caldwell, G.; Magnera, T. F.; Kebarle, P. *J. Am. Chem. Soc.* **1984**, *106*, 959.

(20) Magnoli, D. E.; Murdoch, J. R. *J. Am. Chem. Soc.* **1981**, *103*, 7465. Dodd, J. A.; Brauman, J. I. *J. Phys. Chem.* **1986**, *90*, 3559.

**Table III.** Methyl Cation Affinities

| B | S°(B)[a] | S°($CH_3^+$B)[c] | | $\Delta S°_{13}$ | $\Delta G°_{13}$[l] | $\Delta H_{13}$[m] | $\Delta H$($Me^+$–B)[n] |
|---|---|---|---|---|---|---|---|
| $CH_3Br$ | | | | −2.6[f] | 14.1 | 14.9 | 63.3 |
| $SO_2Cl_2$ | | | | −2[h] | 13.1 | 13.7 | 62.1 |
| $CH_3Cl$ | 56.0 | | | −2.1[f] | 13.0 | 13.6 | 62.0 (64)[y] |
| $CS_2$ | 56.8 | | | 1.6 | 12.3 | 11.8 | 60.2 |
| $SO_2$ | 59.3 | | | −2[h] | 11.6 | 12.2 | 60.6 |
| $CF_3I$ | | | | −1.3[e] | 11.3 | 11.6 | 60.0 |
| $CF_3COCl$ | | | | −2[h] | 10.7 | 11.7 | 60.1 |
| OCS | 55.3 | $CH_3NCS$ | 69.3[d] | 1.6 | 9.3 | 8.8 | 57.2 |
| $CF_3COCF_3$ | | | | −2[h] | 9.5 | 10.1 | 58.5 |
| HBr | 47.5 | | | 4.4[g] | 8.2 | 7.0 | 55.4 (59.8 ± 3)[k] |
| $SO_2F_2$ | 67.7 | | | −2[h] | 6.3 | 6.9 | 55.3 |
| $CH_3F$ | 53.3 | $CH_3OCH_3$ | 63.7 | −2.0 | 5.9 | 6.5 | 54.9 |
| HCl | 44.6 | $CH_3SH$ | 61.0[d] | 4.0 | 4.7 | 3.3 | 51.7 (51 ± 6)[k] |
| $N_2O$ | 52.5 | $CH_3NCO$ | 65.1[b] | 0.2 | 5.1 | 4.5 | 52.9 |
| Xe | 40.5 | $CH_3I$ | 60.7[d] | 7.8 | 4.8 | 2.5 | 50.9 |
| $CF_3Br$ | 73.4[b] | | | −1.3[e] | 4.7 | 5.2 | 53.6 |
| $NF_3$ | 62.3 | $CH_3CF_3$ | 68.7[b] | −6.0 | 4.2 | 6.0 | 53.6 |
| $CF_3Cl$ | 69.0[b] | $CF_3SCH_3$ | 80.3[b] | −1.1 | 4.2 | 4.5 | 52.9 |
| $CO_2$ | 51.1 | $CH_3NCO$ | 65.1[b] | 1.6 | 1.5 | 1.0 | 49.4 |
| $N_2$ | 45.8 | $CH_3CN$ | 58.1[d] | 0 | 0 | 0 | (48.4)[i] |
| Kr | 39.2 | $CH_3Br$ | 58.8[d] | 7.2 | −2.2 | −4.4 | 44.0 |

[a] Entropies at 298 K in cal $mol^{-1}$ $K^{-1}$ from Benson[25] except where otherwise indicated: $\Delta G°_{13}$ at 300 K, $\Delta H°_{13}$, MCA(B), all in kcal/mol. [b] Estimates using group equivalents, Benson.[25] [c] Estimated entropy of $CH_3B^+$ based on entropy for isoelectronic neutral shown. Values for isoelectronic neutrals from Benson[25] except where otherwise indicated. [d] From Stull et al.[26] [e] Assumed the same as $\Delta S°_{13}$ for reaction 13 involving $CH_3Cl$. [f] Assumed the same as $\Delta S°_{13}$ for reaction 13 involving $CH_3F$. [g] Assumed the same as $\Delta S°_{13}$ for HCl. [h] Arbitrary estimate. [i] External standard, Beauchamp et al.,[22] and $\Delta H°_f(CH_3N_2CH_3)$ = 35.5 kcal/mol, Rossini.[22b] [j] Sen Sharma.[27] [k] Estimates based on bracketing literature data leading to PA($CH_3Cl$) ≈ 158 ± 6 kcal/mol and PA($CH_3Br$) ≈ 164.5 ± 3 kcal/mol; see text. [l] Estimated error ±0.5 kcal/mol. [m] Estimated error ±1 kcal/mol. [n] Estimated error ±3 kcal/mol.

**Table IV.** MCA(RCl)[a]

| Me | Et | *i*-Pr | *t*-Bu | eq 17 |
|---|---|---|---|---|
| 62.0[b] | 71[c] | 77[c] | 81[c] | experimental |
| 64.0 | 72 | 79 | 85 | (MINDO/3)[27,28] |

[a] All values in kcal/mol. [b] Experimental result, present work, Table III. [c] Experimental results, Sen Sharma.[27]

Figure 5 and Table III. The generalization that for similar B the reactivity of $MeB^+$ in electrophilic $Me^+$ transfer reactions increases with decreasing MCA(B) may be expected to hold. In summary, the present kinetic results for the $Me^+$ transfer reaction (12) are consistent with the assumption that $-\Delta E_g$ (see Figure 8) and thus the rates, when they are limited by the passage over the barrier, increase with increasing MCA of B and decreasing MCA of B′. The relationship is expected to hold well when series of related B and B′ are involved. Such a series of related B′ would be $CH_3X$ where X = F, Cl, Br, I.

It is notable that these simple relationships, which are easily spotted in the gas phase where the complicating effect of the solvent is absent, can be experimentally demonstrated only when gas-phase ion–molecule reactions with rates lower than collision rates are encountered. Furthermore, in such cases the magnitude of the $\Delta E_g$ can often be determined.[18,19] Knowledge of the values of $\Delta E_g$ allows for the evaluation, via a Born cycle, of the solvation energy of the transition state for the corresponding reaction in solution.[21] This amounts to establishing a quantitative relationships between the reaction in the gas phase and solution.[21]

**c. Thermochemical Data on $Me^+$ Affinities.** The $\Delta G°_2$ results for the $Me^+$ transfer equilibria (2), Figure 5, can be combined to provide a scale giving the $\Delta G°_{13}$ value for the transfer reaction 13. The resulting values for $\Delta G°_{13}$ are given in Figure 5.

$$N_2CH_3^+ + B = N_2 + CH_3B^+ \qquad (13)$$

is the only base for which a good literature value for the MCA is available, and therefore this compound is used as the anchor point (primary standard) of the scale. Beauchamp et al.[22] have measured the photoionization appearance potential of $CH_3N_2^+$ from $CH_3N_2CH_3$. Combining their value with the latest $\Delta H_f°(CH_3N_2CH_3)$ = 35.5 ± 1 kcal/mol, due to Rossini,[22b] one obtains the heat of formation, $\Delta H°_f(CH_3N_2^+)$ = 212.9 kcal $mol^{-1}$. From this value and $\Delta H_f(CH_3^+)$ = 261.2 kcal/mol,[23] one obtains the MCA($N_2$) = 48.3 kcal/mol; see eq 14. This MCA is used

$$N_2CH_3^+ = N_2 + CH_3^+ \qquad \Delta H°_{14} = \text{MCA}(N_2) = 48.3 \text{ kcal/mol}^{22} \qquad (14)$$

in Table III to construct an absolute MCA scale in combination with the results for $\Delta G°_{13}$ from Figure 5. Unfortunately photoionization appearance potentials do not always provide reliable ionic heats of formation so that $\Delta H°_{14}$ could be in error by a few kcal/mol.

Theoretical calculations[24] have established that $CH_3N_2^+$ is linear. Unfortunately the MCA($N_2$) provided by these calculations differ widely depending on the basis set used. Thus, Radom[24a] obtains with STO-3G, 51.6 kcal/mol, in fair agreement with the Beauchamp[22] result, but only 28.5 kcal/mol at the 4-31G level. Simonetta et al.,[24b] using a more flexible basis set which includes polarization functions, obtained the even lower value of 18.4 kcal/mol (for MNDO data, see Ford and Scribner[6]). Obviously, further extended basis set calculations including electron correlation and complete geometry optimization are very desirable.

In order to combine $\Delta H°_{14}$ with the free energy scale $\Delta G°_{13}$ of Figure 5, the $\Delta G°_{13}$ values for the $Me^+$ transfer must be converted to $\Delta H°_{13}$ values. On principle, the $\Delta S°_{13}$ and $\Delta H°_{13}$ could have been obtained by measuring the temperature dependence of the $Me^+$ transfer equilibria (2) and deriving $\Delta H°_2$ and $\Delta S°_2$ from van't Hoff plots. However, since the equilibria 2 were difficult to measure even at one single temperature, this method was not adopted, and instead the $\Delta S°_{13}$ values were estimated. The $S°$(B)'s for most B's available in the literature.[25,26] In a few

(21) Magnera, T. F.; Caldwell, G.; Sunner, J.; Ikuta, S.; Kebarle, P. *J. Am. Chem. Soc.* **1984**, *106*, 6140.
(22) (a) Foster, M. S.; Williamson, A. D.; Beauchamp, J. L. *Int. J. Mass Spectrom. Ion Phys.* **1974**, *15*, 429. (b) Rossini, F. D.; Montgomery, R. L. *J. Chem. Thermodyn.* **1978**, *10*, 465.
(23) Traeger, J. C.; McMoughlin, R. G. *J. Am. Chem. Soc.* **1981**, *103*, 3647.
(24) (a) Vincent, M. A.; Radom, L. *J. Am. Chem. Soc.* **1978**, *100*, 3306. (b) Demontis, P.; Ercoli, R.; Gamba, A.; Suffritti, G. B.; Simonetta, M. *J. Chem. Soc., Perkin Trans. 2* **1981**, 488.
(25) Benson, S. W. *Thermochemical Kinetics*, 2nd ed.; Wiley: New York, 1976.
(26) Stull, D. R.; Westrum, E. F., Jr.; Sinke, G. C. *The Chemical Thermodynamics of Organic Compounds*; Wiley: New York, 1969.

cases $S°(B)$ had to be estimated with the group equivalents method.[25] All the $S°(B)$ data used are given in Table III. $S°(CH_3B^+)$ values were assumed to be the same as those of the isoelectronic neutral. For example, $S°(CH_3N_2^+)$ was assumed to be equal to $S°(CH_3CN)$. $S°(CH_3B^+)$'s and the isoelectronic neutrals used are also given in Table III. $\Delta S°_{13}$ was then calculated from the $S°$ values of the reactants and products. In cases where the $S°$ values of the isoelectronic neutrals were not available, the $\Delta S°_{13}$'s were obtained by assuming that they are identical for homologous pairs. Thus $\Delta S°_{13}$ values for the reactions 15 were

$$N_2CH_3^+ + XCH_3 = N_2 + CH_3XCH_3^+ \quad (X = F, Cl, Br) \quad (15)$$

assumed to be identical. The $\Delta S°_{13}$'s evaluated in this manner were used to obtain $T\Delta S°_{13}$ for $T = 400$ K, and these combined with the PHPMS $\Delta G°_{13}$ led to a $\Delta H°_{13}$ scale. Evaluated $\Delta S°_2$ together with the ICR $\Delta G°_2$ were used to obtain $\Delta H°_2$ values for the compounds determined by ICR; these were then incorporated into the $\Delta H°_{13}$ scale via a common base B in reactions (2) used in PHPMS and ICR determinations. The $\Delta H°_{13}$ scale was then calibrated to the $\Delta H°_1(N_2) = MCA(N_2) = 48.3$ kcal/mol[22] and a $\Delta H_1(B) = MCA(B)$ scale was obtained.

The MCA(B) scale can be checked with available literature data at three points. The $MCA(CH_3Cl) = 63$ kcal/mol based on Sen Sharma et al.[27] and McManus[28] is close to the present value of 61.9 kcal/mol, Table III. Sen Sharma and McManus obtained MCA values from MINDO/3 calculations. The calculations by themselves would not have been convincing; however, Sen Sharma et al.,[27] on the basis of determinations of the temperature dependence of equilibria 16, obtained via van't Hoff plots $\Delta H°_{16}$

$$R^+ + ClCH_3 = RClCH_3^+ \quad (R = Et, i\text{-}Pr, t\text{-}Bu) \quad (16)$$

and from these and thermochemistry data, deduced the experimental MCA(RCl) given in Table IV. The relatively good agreement and consistent trends between the experimental MCA results[27] for RCl = EtCl, *i*-PrCl, *t*-BuCl and the MINDO/3 predicted values[27,28] suggests that the MINDO/3 result for the $MCA(CH_3Cl)$ is too high by $\sim$1 kcal/mol. The experimental and MINDO/3 correlation thus indicates an MCA $(CH_3Cl) = 63 \pm 2$ kcal/mol.

Relationship 17, between the proton affinity of the methyl halide

$$PA(CH_3X) - MCA(HX) = \Delta H_f(H^+) - \Delta H_f(CH_3^+) + \Delta H_f(CH_3X) - \Delta H_f(HX) = 104.5 + \Delta H_f(CH_3X) - \Delta H_f(HX) \quad (17)$$

$CH_3X$ and the $Me^+$ affinity of the corresponding hydrogen halide HX, follows from the definition of the PA and MCA. The value 104.5 kcal/mol for the difference is based on $\Delta H_f(H^+) = 365.7$ kcal/mol and $\Delta H_f(CH_3^+) = 261.2$ kcal/mol.[23]

The proton affinity of $CH_3Cl$ has been established by Beauchamp et al.[15] to be between $PA(C_2H_4)$ and $PA(C_2H_2)$. Using the PA values 162.6 and 153.3 kcal/mol, respectively (Lias[2]), one estimates $PA(CH_3Cl) \approx 158 \pm 6$ kcal/mol which combined with $\Delta H_f(CH_3Cl) = -19.3$ kcal/mol,[29,30] $\Delta H_f(HCl) = -22.1$ kcal/mol,[31] leads via (17) to $MCA(HCl) = 51 \pm 6$ kcal/mol. This can be compared with the present experimental value of 51.7 kcal/mol in Table III.

The proton affinity of $CH_3Br$ has been bracketed[1a] between $PA(C_2H_4) = 162.6$ kcal/mol[2] and $PA(H_2O) = 166.4$ kcal/mol,[2] allowing an assignment of $PA(CH_3Br) \approx 164.5 \pm 3$ kcal/mol. This value combined with $\Delta H_f(CH_3Br) = -8.5$ kcal/mol,[30] $\Delta H_f(HBr) = -8.7$ kcal/mol,[31] leads to $MCA(HBr) = 59.8 \pm 3$ kcal/mol, which can be compared with the present result (Table III) of 55.4 kcal/mol.

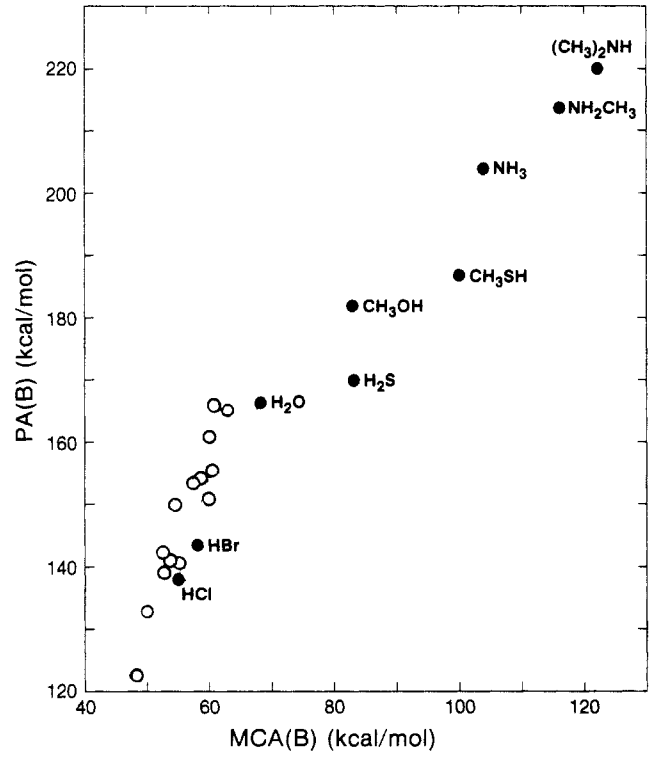


**Figure 9.** Plot of PA(B) vs. MCA(B) including bases B from Figure 8 and bases XH whose MCA(XH) can be evaluated from $PA(CH_3X)$ (see eq 17). Slope changes from $\approx$3 at low MCA(B) to $\approx$1 at high MCA(B): (○) bases from Table III, (●) bases XH.

The above three comparisons with approximate MCA data from the literature are in support of the MCA ladder Table III and suggest an error in the absolute values of approximately $\pm$3 kcal/mol.

Since in Table III MCA(HCl) and MCA(HBr) can be considered more accurate than the bracketed $PA(CH_3Cl)$ and $PA(CH_3Br)$, one can use eq 17 to determine PA values from the MCA. One obtains $PA(CH_3Cl) = 159.0$ kcal/mol and $PA(CH_3Br) = 160.1$ kcal/mol (see also McMahon[31]).

The present MCA scale, Table III, extends to MCA $\approx$ 63 kcal/mol. This is a value somewhat below but close to where the MCA's for oxygen bases like the ethers begin. Thus, from the known heat of formation of protonated dimethyl ether, $\Delta H_f((CH_3)_2OH^+) = 130$ kcal/mol,[2] one can evaluate the $MCA(CH_3OH) = 83.2$ kcal/mol. Therefore, the availability of the present scale holds the promise that future $Me^+$ transfer equilibria measurements to bases with MCA in the 70–80 kcal/mol range will lead to a link up to the numerous conventional oxygen bases and these in turn to the nitrogen bases. Thus, a complete scale of MCA based on equilibria covering a similar range to that available for the PA's[1,2] is made more likely by the availability of the present results.

**d. Relationships between Proton and Methyl Cation Affinities.** Only an approximate relationship between PA(B) and MCA(B) can be expected. When $H^+$ and $CH_3^+$ react with the same basic atom on B, the reaction is formally very similar since it consists of an electron pair donation from B to $H^+$ and $CH_3^+$. The PA(B) should be much larger than the MCA(B) for two reasons. First, the B–H bond formed will be stronger than the B–$CH_3$ bond; second, the electrostatic energy decrease due to the positive charge expansion from the very small $H^+$ to $BH^+$ will be very much larger than that for the expansion from the much bigger $CH_3^+$ to $CH_3B^+$. A more quantitative expression for these factors will be given below.

A plot of PA(B), from Lias,[2] versus the MCA(B) determined in the present work is shown in Figure 8. A fair straight line correlation with a slope $\rho \approx 3$ is observed. In order to examine

(27) Sen Sharma, D. K.; De Hojer, S. M.; Kebarle, P. *J. Am. Chem. Soc.* **1985**, *107*, 3757.
(28) McManus, S. P. *J. Org. Chem.* **1982**, *47*, 3070.
(29) Pedley, J. B.; Naylor, R. D.; Kirby, S. P. *Thermochemical Data of Organic Compounds*, 2nd ed.; Chapman and Hall: London, 1986.
(30) Wagman, D. D., et al. *Selected Values of Chemical and* Thermodynamic *Properties (Technical Note 270-3)*; National Bureau of Standards: Washington, D.C., 1968.
(31) McMahon, T. B.; Kebarle, P. *Can. J. Chem.* **1985**, *63*, 3160.

the relationship over a wider range of data, MCA values for bases of the type HX where X now stands for a basic group like OH, $OCH_3$, etc., were evaluated from thermochemical data[2] with use of eq 17. The extended set is shown in the PA versus MCA plot, Figure 9. It is seen that the bases HX, where they overlap with the data for the general set of bases B, do blend in, i.e., do not form a noticeably distinct line.

The PA versus MCA relationship with the wider range of data, Figure 9, is not a straight line any more. The slope is seen to decrease from $\rho \approx 3$ (low MCA) to $\rho \approx 1$ (high MCA).

Equation 18 can be derived from eq 17 as shown below. The equation is exact only for bases HX; however, a certain interpretative meaning will be obtained from the equation, which is useful also for the general group B. Substitution of the definitions

$$\mathrm{PA(HX) - MCA(HX)} = \mathrm{IE(H) - IE(CH_3) + BE(H\text{–}X) - BE(CH_3\text{–}X) - \Delta PA(CH_3)} \quad (18)$$

for the ionization energies (IE, eq 19), bond dissociation energies (BE, eq 20), and eq 21, which expresses the methyl substituent effect on the proton affinity of HX, into eq 17 leads directly to (18).

$$\mathrm{IE(H)} = \Delta H_f(\mathrm{H^+}) - \Delta H_f(\mathrm{H}) \quad (19)$$

$$\mathrm{BE(H\text{–}X)} = \Delta H_f(\mathrm{H}) + \Delta H_f(\mathrm{X}) - \Delta H_f(\mathrm{HX}) \quad (20)$$

$$\mathrm{\Delta PA(CH_3)} = \mathrm{PA(CH_3X) - PA(HX)} \quad (21)$$

Equation 18 can be given the following qualitative interpretation. As the base is protonated, a charge transfer occurs from $H^+$ to the base (measured by IE(H)) and a bond is formed (measured by BE(H–X). The analogous terms $IE(CH_3)$ and $BE(CH_3–X)$ occur for $CH_3^+$ addition to the base. However, the charge transfer from $H^+$ (or $CH_3^+$) to the base is not complete; therefore, IE(H) and $IE(CH_3)$ are terms that are too large. This "overestimate" is "corrected for" by the methyl substituent effect on the protonation, $\Delta PA(CH_3)$. This term measures the relative energy stabilization of the ion due to some positive charge remaining on the H or $CH_3$.

As the proton affinity of the bases increases, $\Delta PA(CH_3)$ decreases, reaching a small value of a few kcal/mol (see plot of $\Delta PA(CH_3)$ in Figure 10A. This is expected because strongly basic groups (e.g., B = amine) will carry nearly all the positive charge and thus the relative charge remaining on the H or $CH_3$ is not so significant. The very small change of $\Delta PA(CH_3)$ at high PA values is responsible for the near linear region of the PA versus MCA plot in Figure 9, because when $\Delta PA(CH_3)$ becomes constant, PA(HX) and MCA(HX) become linearly related, (see eq 18).

A replot of the PA(B) and the MCA(B) data based on the functional dependence of eq 18 is shown in Figure 10B. The PA(B) – MCA(B) versus PA(B) plot illustrates the asymptotic approach to an approximately constant value at high PA(B) values. This asymptotic region corresponds to the linear region with slope $\rho = 1$ in the PA(B) versus MCA(B) plot in Figure 9.

Since the bond energy difference depends on the nature of the basic atom to which the bond is made, e.g., F, O, N, S, etc., somewhat different asymptotic values are expected for series of bases with a given basic atom. Thus, two high PA limits are observed in Figure 10b, the higher one corresponding to the nitrogen bases and the lower one to the sulfur bases. It will be interesting to see how the plot will look when MCA data for general bases B and not only for bases XH become available in the high affinity range.

**e. Unique Features of Individual Methyl Cation Affinities. (i) Rare Gases.** Methylated rare gas cations have previously been observed by Field et al.[32] as ions of very low abundance in electron impact studies of $CH_4$/rare gas mixtures at high pressures in a conventional mass spectrometer. However, the means of formation of these species was not identified nor were any data obtained

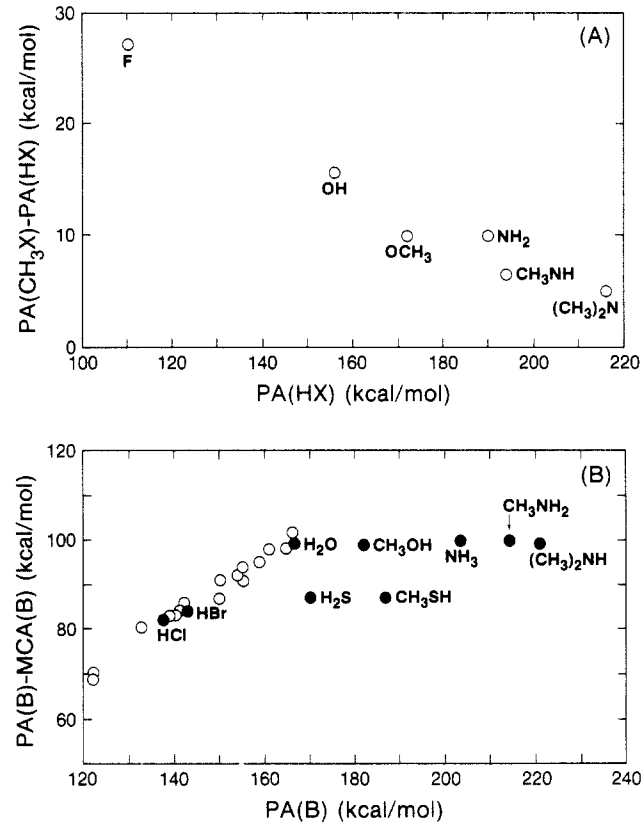


**Figure 10.** (A) Plot of $PA(CH_3X) - PA(HX)$ for X groups shown. (B) Plot of PA(B) – MCA(B) versus PA(B) reaches a constant value at high PA(B): (○) bases from Table III, (●) bases HX.

regarding their energetics. Reaction of $Kr^+$ with $CH_4$ at superthermal kinetic energies in a chemical accelerator study demonstrated the formation of $CH_3Kr^+$.[33] Based on ICR observations of methyl cation transfer equilibria, Hovey and McMahon[11,12] assigned methyl cation affinities of 51.5 ± 3 and 44.5 ± 3 kcal/mol for Xe and Kr, respectively.[34] Based on correlations of methyl cation affinity with proton affinity, it was further suggested that the methyl cation affinity of Ar should be ~41 kcal/mol and might therefore be observable by $CH_3^+$ transfer from $CH_3FH^+$.

**(ii) $CO_2$.** Holmes et al.[35] have carried out collisional activation and metastable observation experiments on a variety of $C_2H_3O_2^+$ ions including $CH_3OCO^+$. In addition, ab initio calculations and appearance energy measurements were used to determine $\Delta H°_f(CH_3OCO^+)$. Based on an appearance energy of 11.24 eV for $CH_3OCO^+$ from $ClCO_2CH_3$ a value of $\Delta H°_f(CH_3OCO^+)$ of 126 kcal/mol was obtained corresponding to a methyl cation affinity of $CO_2$ of 41 kcal/mol. However, metastable peak observations indicated that formation of $CH_3OCO^+$ from $ClCO_2CH_3^+$ involves a significant reverse activation energy, establishing 41 kcal/mol as a lower limit to the methyl cation affinity of $CO_2$. Ab initio calculations yielded $\Delta H°_f(CH_3OCO^+)$ as 120 kcal/mol and a methyl cation affinity of $CO_2$ of 47 kcal/mol. However, the calculation did not involve a complete geometry optimization. Therefore, the value of 49.5 kcal/mol obtained in the present work appears to be quite reasonable and in agreement with the above results.

**(iii) $NF_3$.** Recent studies of protonation of $NF_3$ by both ion cyclotron resonance and ab initio techniques have demonstrated that the most favorable site of protonation of $NF_3$ is at fluorine

(32) Field, F. H.; Head, M. H.; Franklin, J. L. *J. Am. Chem. Soc.* **1962**, *84*, 1118.

(33) Wyatt, J. R.; Stratten, L. W.; Hierl, P. M. *J. Phys. Chem.* **1976**, *80*, 2911.

(34) The MCA values quoted[11,12] were higher by 3.5 kcal/mol. This was due to use of Beauchamp's[22a] $AP(CH_3N_2^+)$ in combination with an older and less reliable value for $\Delta H°_f(CH_3N_2CH_3)$.

(35) Blanchette, M. C.; Holmes, J. L.; Hop, C. E. C. A.; Lossing, F. P.; Postma, R.; Ruttink, P. J. A.; Terlow, J. K. *J. Am. Chem. Soc.* **1986**, *108*, 7589.

rather than nitrogen.[36] As a result consideration must be given to possible methylation of $NF_3$ at both sites as well. A collision-induced decomposition experiment involving the $CH_3NF_3^+$ ion, derived from $CH_4/NF_3$ mixtures in the CI source of a reverse geometry double-focusing instrument, showed dominant loss of $CH_3F$ to yield $NF_2^+$ and of $NF_2H$ to yield $CH_2F^+$. These data are consistent with initial attachment of $CH_3^+$ to a fluorine of $NF_3$, eq 22. During the chemical activation process, an N–F bond

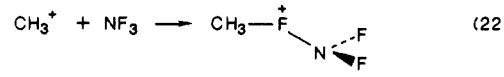

(22)

may be cleaved, leading directly to $NF_2^+$, or a tight ion–molecule complex may be formed ($CH_3F + NF_2^+$) from which $NF_2^+$ may insert in a C–H bond of $CH_3F$ with subsequent unimolecular decomposition giving rise to $CH_2F^+ + NF_2H$. $NF_2^+$ has previously been shown[36] to readily insert into C–H bonds.

**(iv) $N_2O$.** $N_2O$ is isoelectronic with $CO_2$ and has a greater basicity toward both $H^+$ and $CH_3^+$, and again the possibility of ambidentate character must be considered. In a high resolution infrared study of gaseous protonated $N_2O$, Amano[37] concluded that protonation takes place predominantly on oxygen. Collision-induced decomposition studies reveal evidence of both possible protonated forms of $N_2O$; however, CID of methylated $N_2O$ was more strongly suggestive of methylation at nitrogen since the major fragmentation under CID conditions led to $NO^+$.[36]

**(v) $SO_2F_2$ and $SO_2$.** Both $SO_2$ and $SO_2F_2$ have frequently been used as solvents of low nucleophilicity in the study of superacids.[38] Gillespie has shown that solutions of $CH_3F/SbF_3,SO_2$ lead readily to formation of a new ionic species, $CH_3OSO^+$, which can be characterized by both NMR and X-ray crystallographic techniques.[39] Both Gillespie[40] and Olah[41] have demonstrated that $SO_2F_2$ is a much more weakly coordinating solvent so that no $CH_3OSOF_2^+$ is formed, leaving only $CH_3^+SbF_6^-$ complexes in $SO_2F_2$ solution. This is in agreement with the present data which show $SO_2$ to bind $CH_3^+$ more strongly than $SO_2F_2$ by 5 kcal mol$^{-1}$. The comparable gas-phase basicities of $SO_2F_2$ and $CH_3F$ toward $CH_3^+$ further suggest that under favorable conditions the dimethylfluoronium ion, $(CH_3)_2F^+$, might be observable by NMR. The present methyl cation affinity scale also provides useful suggestions for other potential solvents for "magic methyl" experiments.

**(vi) OCS and $CS_2$.** The similarity of the methyl cation affinities of COS and $CS_2$ and the larger difference between those of $CO_2$ and OCS suggest that OCS methylates at sulfur. The comparable methyl cation affinities of $CS_2$ and $SO_2$ also indicate that $CS_2$ might usefully be exploited as a solvent in superacid systems where it is desirable to work at temperatures above the liquid range of $SO_2$. To the best of our knowledge no such attempts have been made.

**(vii) $(CF_3)_2CO$ and $CF_3COCl$.** The trifluoromethyl group is known to significantly weaken the C=O bond as evidenced by the substantially lower stretching frequency for these carbonyls compared to that in $(CH_3)_2CO$. This leads to a reduced basicity of $CF_3$ substituted compounds relative to their pure hydrogenic analogues. This reduction in basicity and the slightly lower methyl cation affinity of $CF_3COCl$ relative to $CH_3Cl$ give rise to the possibility that $CF_3COCl$ may, in fact, be a chlorine, rather than oxygen, base toward $CH_3^+$.

**Acknowledgment.** This work was supported by the Natural Sciences and Engineering Research Council of Canada (NSERC).

**Registry No.** $Me^+$, 14531-53-4; $Me_2F^+$, 64710-12-9; $CH_3Cl$, 74-87-3; $CS_2$, 75-15-0; $SO_2Cl_2$, 7791-25-5; $SO_2$, 7446-09-5; $SO_2ClF$, 13637-84-8; $(CF_3)_2CO$, 684-16-2; $Me_2Cl^+$, 24400-15-5; $(CH_3)_3N$, 75-50-3; $NH_3$, 7664-41-7; $(CH_3)_2O$, 115-10-6; $C_2H_5OH$, 64-17-5; $CH_3C_6H_5$, 108-88-3; $C_6H_6$, 71-43-2; $CH_3Br$, 74-83-9; $CF_3I$, 2314-97-8; $CF_3COCl$, 354-32-5; OCS, 463-58-1; BrH, 10035-10-6; $SO_2F_2$, 2699-79-8; $CH_3F$, 593-53-3; ClH, 7647-01-0; $N_2O$, 10024-97-2; Xe, 7440-63-3; $CF_3Br$, 75-63-8; $NF_3$, 7783-54-2; $CF_3Cl$, 75-72-9; $CO_2$, 124-38-9; $N_2$, 7727-37-9; Kr, 7439-90-9.

(36) Fisher, J. J.; McMahon, T. B. *J. Am. Chem. Soc.*, following paper in this issue.
(37) Amano, T. *Chem. Phys. Lett.* **1986**, *127*, 101. Amano, T. *Ibid.* **1986**, *130*, 154.
(38) Olah, G. A.; Surya Prakash, G. K.; Sommer, J. *Superacids*; Wiley: New York, 1985.
(39) Gillespie, R. J.; Riddel, F. G.; Slim, D. R. *J. Am. Chem. Soc.* **1976**, *98*, 8069.
(40) Calves, J. Y.; Gillespie, R. J. *J. Am. Chem. Soc.* **1977**, *99*, 1788.
(41) Olah, G. A.; Donovan, D. J. *J. Am. Chem. Soc.* **1978**, *100*, 5163.